A novel hybrid method for predicting vertical levelling loss of railway track geometry under dynamic cyclic loadings

Oliveira De Melo, Andre; Kaewunruen, Sakdirat; Papaelias, Mayorkinos; Li, Ting

DOI:
10.1142/S0219455422501620

Document Version
Peer reviewed version

Citation for published version (Harvard):
Oliveira De Melo, A, Kaewunruen, S, Papaelias, M & Li, T 2022, 'A novel hybrid method for predicting vertical levelling loss of railway track geometry under dynamic cyclic loadings', *International Journal of Structural Stability and Dynamics*, vol. 22, no. 14, 2250162. https://doi.org/10.1142/S0219455422501620

International Journal of Structural Stability and Dynamics

A novel hybrid method for predicting vertical levelling loss of railway track geometry under dynamic cyclic loadings

Andre Luis Oliveira de Melo

School of Engineering, University of Birmingham, Birmingham, B15 2TT, United Kingdom
alo888@student.bham.ac.uk

Sakdirat Kaewunruen*

School of Engineering, University of Birmingham, Birmingham, B15 2TT, United Kingdom
s.kaewunruen@bham.ac.uk

Mayorkinos Papaelias

School of Metallurgy and Materials, University of Birmingham, Birmingham, B15 2TT, United Kingdom
m.papaelias@bham.ac.uk

Ting Li

School of Railway Engineering, Southwest Jiaotong University, Chengdu, 611756, China
liting9225@126.com

Received Day Month Year
Revised Day Month Year

With an emphasis on the integrated deterioration of railway track geometry and components, a new hybrid numerical-analytical method is proposed for the predictive analysis of track geometrical vertical levelling loss (VLL). In contrast to previous studies showing a dependency on the number of cycles, this research unprecedentedly incorporates the influence of operational, vehicle and track conditions. The numerical models are carried out using an explicit finite element (FE) package under cyclic loadings, and then, their outcomes are iteratively regressed by an analytical logarithmic function that accumulates permanent deformations in order to quantify VLL over a long term. The results are first compared with other previous studies, indicating a very good agreement with them. Then, field measurements have been used to further verify the results. In this study, parametric simulations are performed varying three key parameters: axle load, train velocity and ballast tangent stiffness. The parametric studies exhibit that the rate of VLL raises about 50% if the axle load increases only from 30 to 40 tonnes for a freight train running at 70 km/h on a stiffer ballast track. In contrast, for a 25-tonnes-axle-load train running from 60 km/h to 100 km/h on a similar track, the vertical levelling degradation reduces by approximately 20%. The main findings suggest that higher axle loads contribute significantly to the VLL due higher contact forces and, on the other hand, a lower train speed does not necessarily imply a low rate of VLL since the influence of train velocities on track geometry (VLL) is associated with the natural frequencies (or wavelengths) of the ballasted railway track. The insight demonstrates that the load frequencies play a key role on the deterioration of VLL.

* Correspondent author: s.kaewunruen@bham.ac.uk.

Keywords: Track degradation; track geometry; vertical levelling loss, ballast elastic-plastic behaviour; cyclic loading; Finite Element Method (FEM).

1. Introduction

Post-construction degradation of track geometry is one of the major issues for railway track maintenance.[1] Increasing demands for higher velocities, heavier axle loads, and more frequent rail transport can accelerate rapidly this degradation due to cyclic traffic loadings.[2] An important contribution to this degradation is the differential track settlement, which impacts directly on the spatial position of the rail track, defined as vertical levelling that is one of the most important track geometry parameters. A poor vertical profile means a poor ride quality and excessive dynamic forces for track and vehicles components, and the inevitable result is a less efficient, less popular and more costly railway.[3]

The vertical levelling of railway track geometry refers to the adherence to established grade and uniformity of both transversal and longitudinal directions in the plane across the heads of the two rails.[4,5] Also known as vertical profile or longitudinal level,[6] it is the deviation Z_p', of consecutive running table (1) levels on any rail, expressed as an excursion from the mean vertical position (reference line - 2), which are shown schematically in Figure 1. Any weakness in the support system (track components) – subgrade, reinforcement of the subgrade, sub ballast, ballast, sleeper, fastening system and rail – will affect adversely the railway track vertical profile. Furthermore, according to Ref. 4, it is important to understand that good vertical levelling applies to the track in its loaded rather than unloaded position.

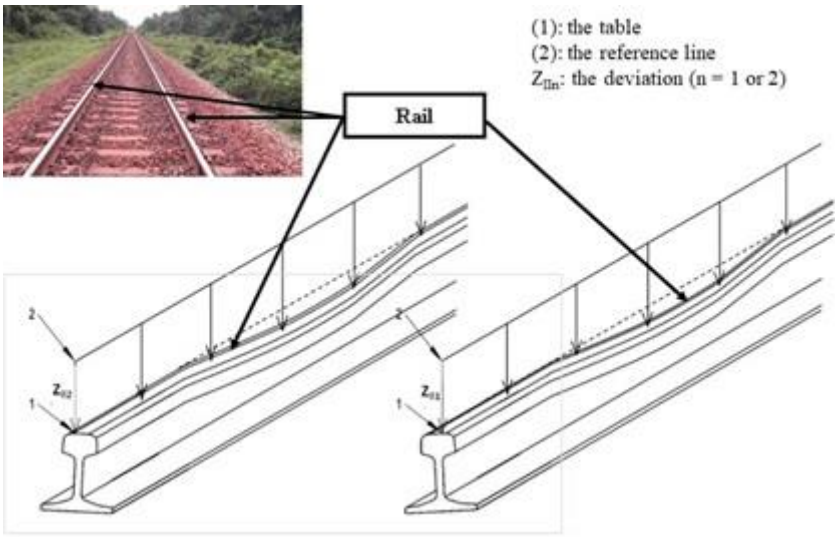

Fig. 1. Vertical levelling parameter of railway track geometry (Adapted from Ref. 6).

In principle, the vertical levelling loss (VLL) of track geometry or, in other words, how much the rail losses its vertical position in the railway track physical space, can be described to occur in two phases before the first maintenance intervention. In the first phase directly after track construction or maintenance there is a rapid consolidation of the ballast. The second phase, there is a slower loss rate related slightly to flattened and worn rail, damaged rail pad, and largely to ballast, sub ballast and subgrade settlement in the short-term performance. At this stage, the rate can be generally approximated by a linear degradation with the logarithm of the number of cyclic loadings. This is in accordance with Ref. 7 who describes that the rate of ballast plastic deformation decreases gradually as cyclic loadings increase indicating also a logarithmic behaviour for VLL. As the ballast has the largest influence on track settlements according to Ref. 8 and Ref. 9, this study also pays special attention to the track component. Additionally, over a long term, there are further settlements due to ballast particle rearrangements and particle breakdowns as well as penetration of sub-ballast and subgrade into ballast voids and inelastic recovery of subgrade at unloading.[2] Moreover, as highlighted in Ref. 10, Ref. 11, Ref. 12, and Ref. 13, the railway track structure and its components, particularly the ballast (however, it can also be extended to the sub ballast and subgrade), play an important role in being dynamically affected by the load travelling velocity and, consequently, having a different amplification of its displacement depending on how it vibrates naturally. In other words, the natural frequencies in which a specific track vibrates influence on how much the ballast deflects under a specific train velocity[14,15,16] over time, which can negatively affect its critical train velocity. Figure 2 depicts a typical heavy haul railway track in a straight segment with its components and, in details, the register of ballast particle breakdowns after tamping the track.

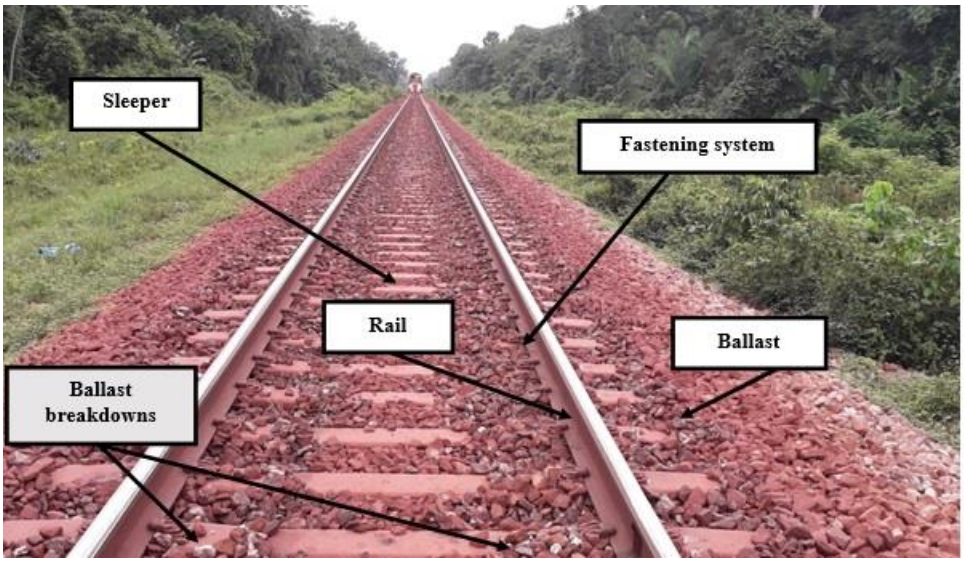

Fig. 2. Typical single railway track and some of its components.

A large number of VLL predictive approaches have been derived empirically (directly or indirectly) from laboratory (triaxle, reduced scaled box or full-scale box tests) and field experiments, by various researchers worldwide, mostly focusing on ballast settlement. Ref. 17 carried out an excellent critical review, which was mentioned by Ref. 3, and updated and well-illustrated recently by Ref. 18. Figure 3 summarize the comparison of these approaches graphically. It can be noted that those VLL investigations are presented within three different ranges of initial ballast compaction: softer, medium and stiffer, respectively '1-5 mm', '5-10 mm', '> 10 mm', for 900 thousand cycles. However, based on that updated review, it is possible to infer that there is not a consensus among the experimental conditions under which the experiments were performed and, hence, among the results. This means clearly that there is a research gap related to the specification of numerical and field (or laboratory) experiments to coordinate or harmonise the VLL predictions. Moreover, mostly empirical methods indicate a dependency exclusively on the number of cycles without taking into account any different operational, environmental, vehicle, and track conditions. In order to address those two knowledge gaps identified, this study proposes the development of a new hybrid numerical-analytical method considering railway dynamic conditions.

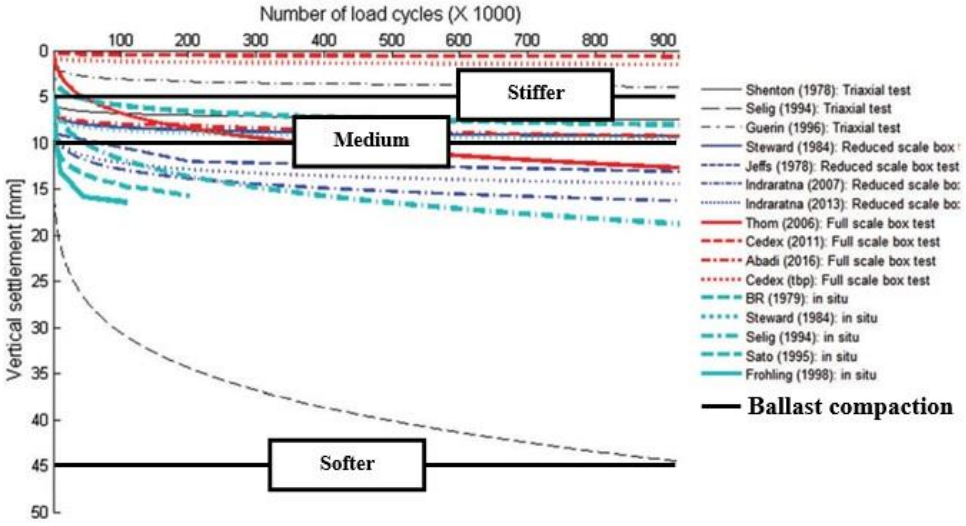

Fig. 3. Comparison of ballast empirical settlement predictive laws from laboratory and field experiments (Adapted from Ref. 18).[3,8,19-27,41]

The development of a new hybrid method to predict track geometry VLL can be extremely useful for filling the current knowledge gap (especially when considering the global train-track dynamics) and, consequently, improving the planning, decision-making and maintenance activities. According to Ref. 28 and Ref. 29, different approaches of track degradation models have been continuously developed over the past few years, however

there are still many vehicle-track related issues that are not fully understood. The plastic deformation and non-linearity including material properties, geometry and contacting surfaces, under cyclic loadings, are some of these issues to be addressed as also identified by Ref. 30.

In this study, a nonlinear numerical modelling has been proposed to predict the train-track interactions, and later an analytical method has been integrated to estimate VLL, under heavy haul dynamic cyclic loadings, which can also embrace the train-track dynamics. It is important to note that previous studies are rather limited to a dependency on the number of cycles or million gross tonnes (MGT) and cannot be generalized. On this ground, this study further embraces the influence of dynamic and operational conditions, track components and vehicle parameters. Accordingly, short- and long-term behaviours of a ballasted track can be analysed to determine parametric effects on the track geometry VLL. With the increase in computing power and speed, it will be possible to adopt a more complex model of track geometry elements incorporating a diverse dynamic railway environment. This can enhance predictive maintenance for both track geometry degradation and component deterioration[31].

2. Methodology

Our numerical study is performed considering the technical and operational characteristics of the Carajas Railway (EFC), one of the most important heavy haul railway in Brazil that is planning to transport more than 240 million tonnes of iron ore, mainly, and soil bean. Its track has 1600 mm gauge and is composed by ASTM 136RE rail (weight: 68 kg/m), mono-block concrete sleeper (length: 2800 mm, height: 250 mm and width: 265 mm), spacing between sleepers of 610 mm, e-clip fastening system and crushed rock ballast (height: 300 mm and shoulder: 300 mm). In the EFC, the key railway vehicle is the GDE wagon of which the distance between axles and the adjacent bogies are 1828 mm and 2562 mm, respectively, considering this configuration of the bogies as the greatest load solicitation due to the effect of superposition that the wheel loads cause into the track.[32,33] In this study, a straight segment is chosen as the initial focus is on vertical levelling of the track geometry. As different types of finite elements (FE) enable a variety of structures or components, the EFC's track can be modelled in both two and three dimensions. Based on the typical track and vehicle components illustrated in Figures 2 and 4, respectively, and their parameters described on Table 1, the model is designed in 3D on LS-Dyna, a commercial FE software package, for modelling approximately 25 meters of railway track and two halves of the typical wagon. The model is performed by applying both linear elastic and elastic-plastic behaviours of the materials to investigate the effect of axle loads, ballast parameters and train velocities on VLL over time. This nonlinear model uses an advanced moving mass loads to represent the vehicles, which travel in loop along perfect track geometry as shown in Figure 5. To perform the designed model, the High-Performance Computing (HPC) facilities have been used through the BlueBEAR platform.

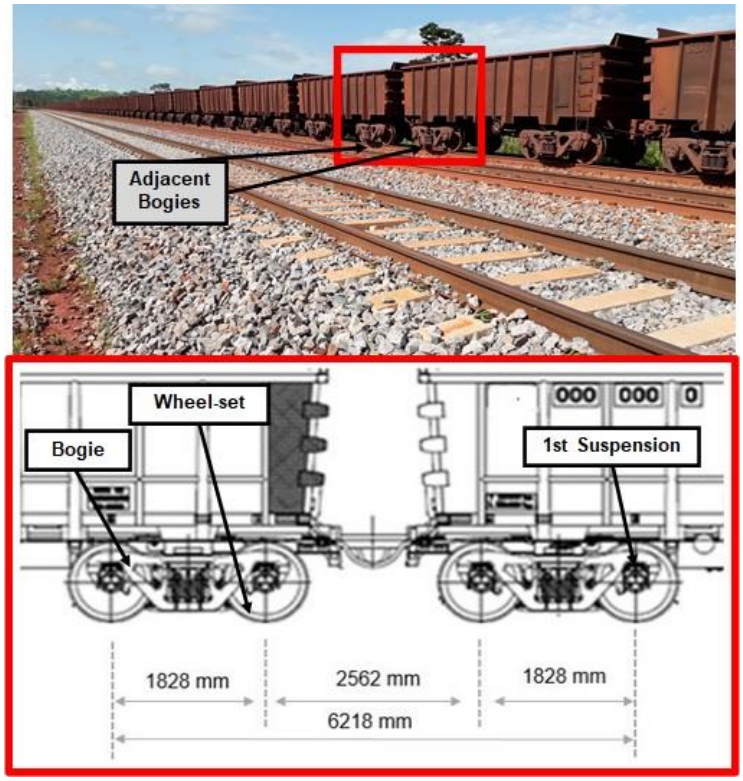

Fig. 4. Typical railway vehicle in the EFC: (a) two iron ore wagons, and in details (b) the vehicle model configuration illustrating the adjacent bogies and its components (Adapted from Ref. 32 and Ref. 33).

Table 1. Track and vehicle parameters in the EFC (Adapted from Ref. 32 and Ref. 34)

Track Component	Type	Constitutive Material	Finite Element	Parameter(s)
Rail	136RE	Elastic	Beam	Density: 7.85e-9 ton/mm^3 Young's Modulus: 2e5 N/mm^2 Poisson's Ratio: 0.3
Sleeper	Mono-block concrete	Elastic	Beam	Density: 2.5e-9 ton/mm^3 Young's Modulus: 4.3e4 N/mm^2 Poisson's Ratio: 0.15
Fastening System	E-clip and rail pad	_astic	Spring	Elastic Stiffness: 1.7e5 N/mm
Ballast	Fresh well-stabilized crushed rock	Elastic-plastic	Spring and Damper	Elastic Stiffness: 45.43 MN/mm Yield Force: 500 N Tangent Stiffness: 500 N/mm Damping constant: 3.2 N/mm

Table 1 (continued).

Track Component	Type	Constitutive Material	Finite Element	Parameter(s)
Sub Ballast	A- (TRB)	Elastic	Solid	Density: 1.7e-9 ton/mm^3 Young's Modulus: 400 N/mm^2 Poisson's Ratio: 0.33
Reinforcement of the Subgrade	ND	Elastic	Solid	Density: 1.5e-9 ton/mm^3 Young's Modulus: 160 N/mm^2 Poisson's Ratio: 0.36
Subgrade	ND	Elastic	Spring	Elastic Stiffness: 1 kN/mm
Vehicle Component	Type	Constitutive Material	Finite Element	Parameter(s)
Wheel Set	6 ½" X 9", wheel diameter: 965 mm	Rigid	Beam	Density: 7.85e-9 ton/mm^3 Young's Modulus: 2e5 N/mm^2 Poisson's Ratio: 0.30
1st Suspension	ND	Elastic	Spring and Damper	Elastic Stiffness: 1.751e8 N/mm Damping Constant: 3.502e3 N.s/mm
Bogie	Ride Control	Rigid	Shell	Density: 7.85e-9 ton/mm^3 Young's Modulus: 2e5 N/mm^2 Poisson's Ratio: 0.3

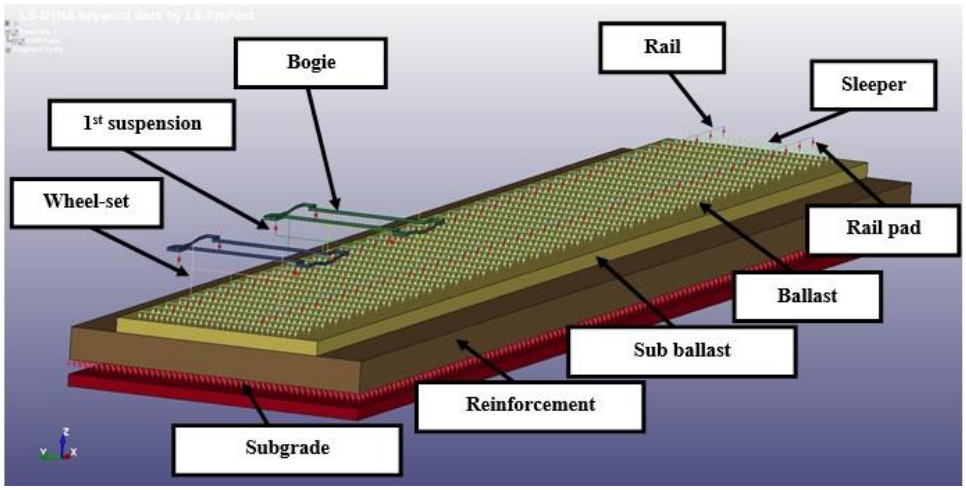

Fig. 5. EFC's railway track and vehicle model on LS-Dyna FE software.

In most ballasted railway tracks, it is known that the ballast settlement is the main source of VLL. According to Ref. 8, there are three necessary conditions for that: (i) existence of filter/separation layer between the coarse ballast and fine subgrade, (ii) a sufficiently strong subgrade or reinforcement of the subgrade / subgrade combination, and (iii) good drainage of water entering from the surface. These conditions have been assumed in this study to model the track. Additionally, the ballast is a gravel-size crushed rock that forms the top layer of the railway track structure, in which the sleeper is embedded and supported,[35] and it is subjected to a uniquely severe combination of loading stresses and environmental exposure, under cyclic loadings. As a granular layer, its deformation can be due to particle rearrangement to a denser packing and particle breakage with the smaller particles moving into the voids of the larger particles. This vertical cumulative deformation of the ballast is considered and may be approximately represented on FE model as an elastic-plastic discrete element with isotropic hardening. It has a bilinear force-displacement relationship that is specified by elastic stiffness, a tangent stiffness and a yield force, as illustrated in Figure 6, and in which the applied load is split into a sequence of increments (cyclic loadings). The force-displacement relation during cyclic loading can be written as:

$$f\hat{} = F_y * (1 - K_t / K_e) + K_t * \Delta l \tag{2.1}$$

where $f\hat{}$ is the actual force, F_y is the yield force, K_e is the elastic stiffness and K_t is the tangent stiffness.

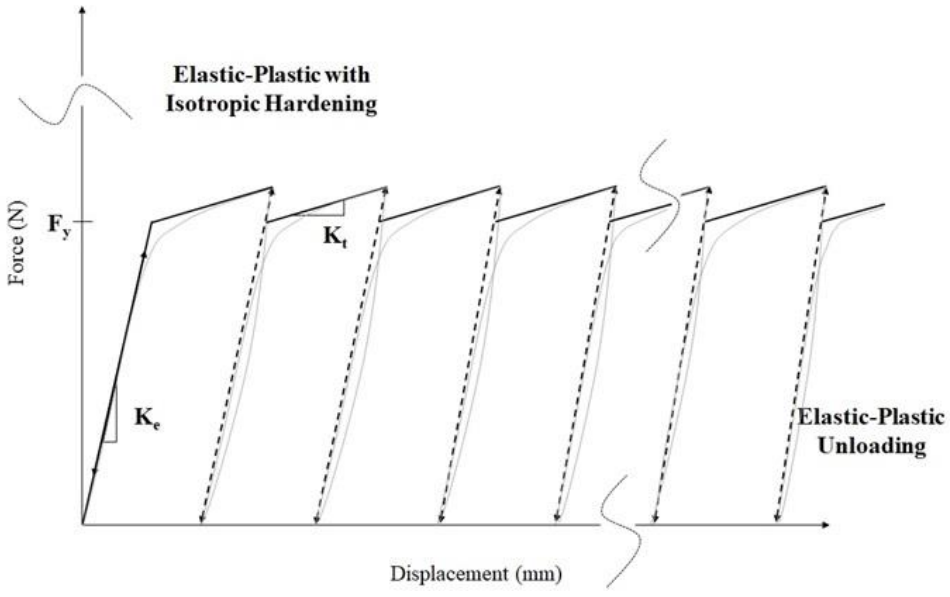

Fig. 6. Loading and unloading force-displacement curves for considering the ballast elastic-plastic behaviour.

On the other hand, over a period of time, the ballast voids become progressively filled with not only fine particles (fouled) from the particle breakage, but also, for example, fine particles that fall down from iron ore loaded wagons during railway traffic. According to Ref. 35, the deterioration of ballast is expected to produce a reduced frictional resistance between the particles than the value of a fresh ballast. Adding this to the modification of ballast state as mentioned before, the ballast track parameters change after a number of cyclic loadings, however, it is not taken into account in this modelling.

It is important to highlight that it is very difficult to translate the real track conditions to a numerical study. To overcome partially these challenges, a methodology to develop this study is indicated in Figure 7. Previously, a wide range of literature had been reviewed regarding track geometry degradation.[30] The research also analyses the collected data from railway companies in Brazil, defines some assumptions and limitations of the study, designs the numerical studies (the railway track and vehicle model), and performs and provides the validation of the model, under different cyclic loadings conditions. Following on from this study, performance and analysis of the long-term behaviour of the model are presented, dependent variables are identified and final graphics to predict the track geometry VLL, under different parameters, are proposed.

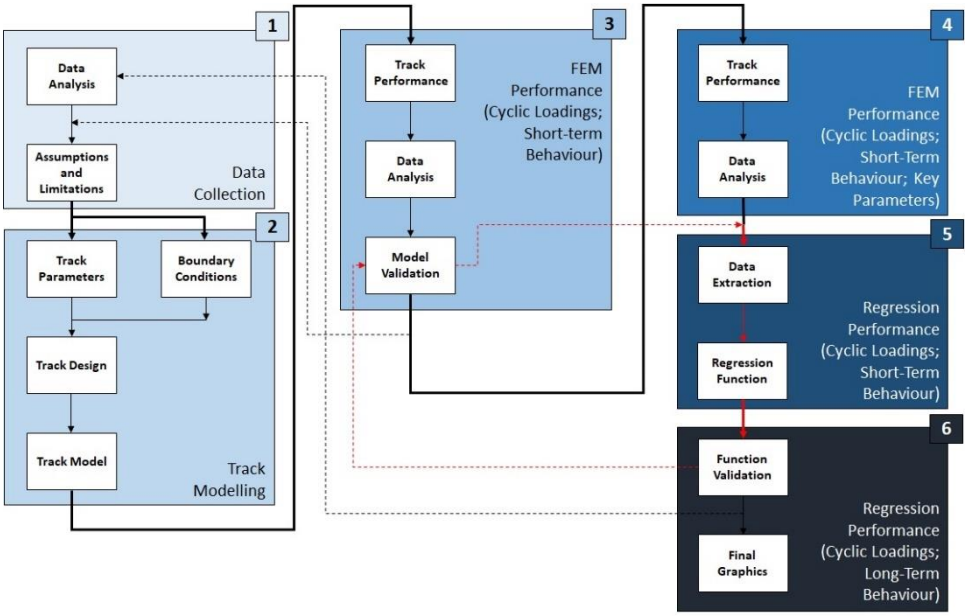

Fig. 7. Methodology flowchart.

One of the key challenges to be addressed by this study is associated with the residual (permanent or plastic) ballast settlement which is extremely small (in the order of a nanometer) with each cyclic loading. Another issue to be overcome is related to the computational effort to perform the model. Despite the fast development of computing

tools, the numerical solving is affected by computational time limitations. To solve this issue, a mass scaling to increase the time step duration in each cycle[36,37] and a time scaling computed on a shorter load step in loop are implemented. It is also assumed that the response in a shorter load step is a good representation of the behaviour in real loadings – this is validated by other studies[4,7,8,38,39], and the material properties do not change with the number of load cycles, which is a limitation of this model.[40]

Initially, the numerical study is carried out using LS-Dyna and the maximum values of vertical rail displacement (VRD), under cyclic loadings, are numerically generated by the nonlinear FE model. Consecutively, the maximum values of VRD under cyclic loadings (short-term behaviour) are extracted, plotted and regressed by a Nepierian logarithmic function to provide an analytical estimation of the maximum VRD for the real cyclic loadings as stated earlier. This equation can be written as:

$$Max_{VRD} = a*ln(N) + b \tag{2.2}$$

where 'Max_{VRD}' is the maximum vertical rail displacement, 'a' is the rate of 'Max_{VRD}', 'N' is the number of cyclic loadings, and 'b' is the initial rail displacement.

After this initial investigation, the differences between each 4-cycle loads into the long-term behaviour (< 6 MGT) of Max_{VRD} regressed function (Eq. 2.2) are calculated. The results indicate the first term of that regressed function as the track geometry VLL, which also may be written as:

$$VLL = a_{VLL}*ln(N) \tag{2.3}$$

$$VLL = a_{VLL}**ln(T/W) \tag{2.4}$$

where 'VLL' is the vertical levelling loss, 'a_{VLL}' the rate of 'VLL', 'N' is the number of cyclic loadings, 'T' is million gross tonnes (MGT) and 'W' is the axle load (in tonnes).

Eq. 2.3 provides an estimation of the cumulative VLL for the real cyclic loadings. Such the result is also compared to the triaxle experiments under repeated loadings carried out by Ref. 32 at the same operational and track conditions as aforementioned. Additionally, different operational and track characteristics are applied to the verified model and the outcomes are also compared to the studies provided by Ref. 39 and Ref. 41. This stage is related to the model validation as indicated in Figure 7.

After validating the track model under cyclic loadings, the simulations continue being performed – Stage 4 – varying three key parameters: axle load (15-40 tonnes, light to heavy haul loadings), train velocity (60-160 km/h, low to medium speeds) and ballast tangent stiffness (300-500 N, softer to stiffer ballast plastic deformations). The results are also extracted and analyzed, and differ to the previous stage – the model validation, not only the rates of VLL are identified but also they are plotted to evaluate both the behaviour of VLL and the influence of those three different parameters on it. Furthermore, the final

graphics explicitly indicate a predictable behaviour of VLL on rail track surface (wheel-rail contact) to those dynamic characteristics, under cyclic loadings.

3. Results and Discussion

To examine whether the numerical model can provide reliable insight into the VLL, first the validity of the FEM outcomes regarding the VRD in short-term cyclic loadings have to be investigated. Subsequently, it is addressed a short-term regression function before analyzing the long-term behaviour of VLL. Figure 8 illustrates the model performed using LS-Dyna FE package.

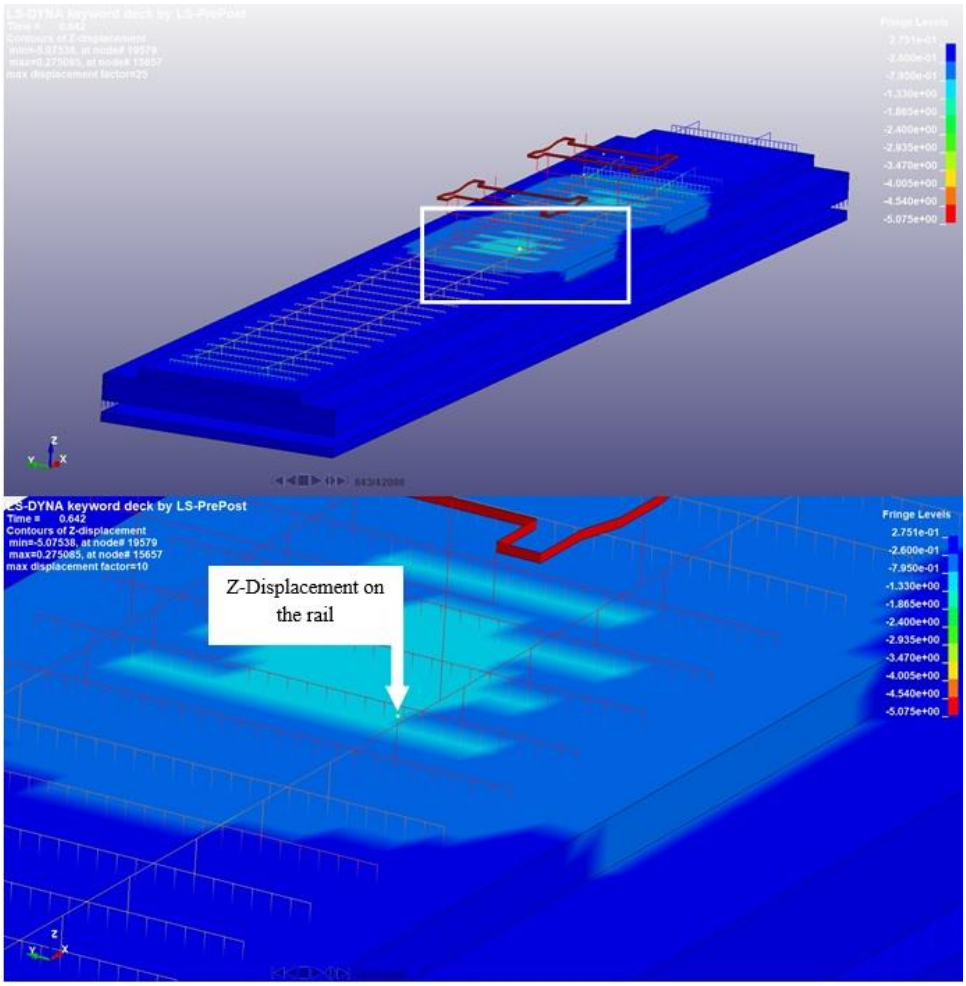

Fig. 8. Track model performed, under 20-tonnes axle load, 70-km/h train velocity, and 500-N/mm ballast tangent stiffness (in details – bottom, the rail FE node displacement just after the fourth load cyclic).

Initially, the track model under 368 cyclic loadings (approximately 100s of a shorter loading step in loop) and operational parameters of 20-tonnes axle load and 70-km/h train velocity is performed on HPC. Figure 9 depicts the VRDs after being extracted and plotted in a time-domain graphic.

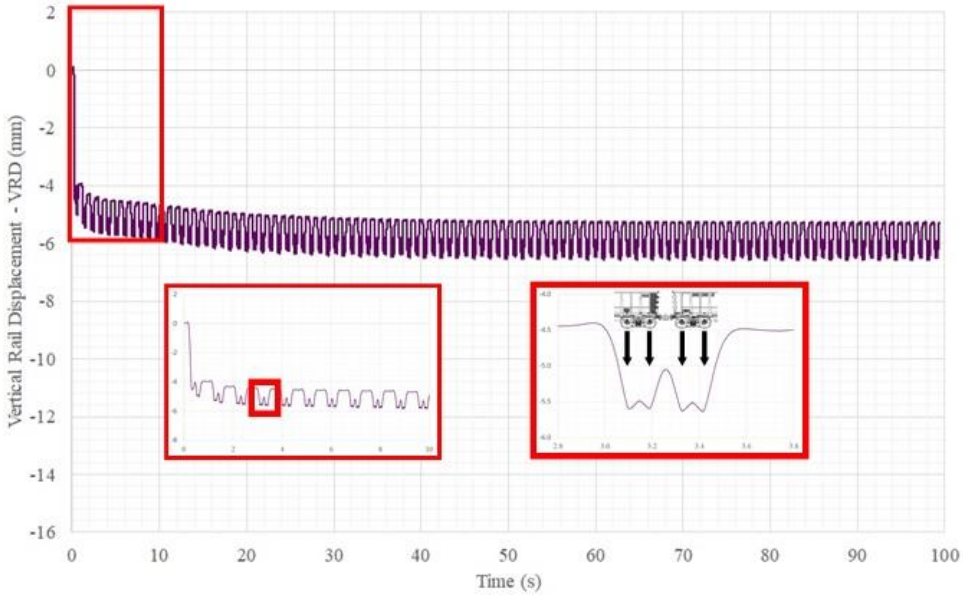

Fig. 9. Short-term behaviour of VRDs on FEM under 20-tonnes axle load, 70-km/h train velocity and 500-N/mm ballast tangent stiffness (in details, left: the initial vertical rail displacements, and right: the effect of superposition caused by the wheel loads).

The VRDs are computed by the summation of elastic-plastic displacement between the wheel and the rail in vertical direction ('Z-Displacement' in Figure 8) for each load applied. It is well-known that the largest VRDs occur during the first cyclic loadings and correspond mainly to the process in which the gaps between ballast particles are unified and consolidated.[42] This initial ballast consolidation is considered to depend on both the work done on it (i.e., the axle load and, consequently, the contact force between the track components) and the ballast parameters, particularly the ballast tangent stiffness. A similar trend of VRDs can be found in Figure 9, in which the slope of those displacements is likely to represent how faster and deeper the railway track loses its vertical levelling. The maximum VRD (Max_{VRD}) immediately after each 4 cycles (a half loop) of those cyclic loadings are identified and plotted in a 'Number-of-Cyclic-Loadings (un) x VRD (mm)' graphic to support the next step of this analysis. Figure 10 illustrates the Max_{VRD} values under 20-tonnes axle load, 70-km/h train velocity and 500-N/mm ballast tangent stiffness.

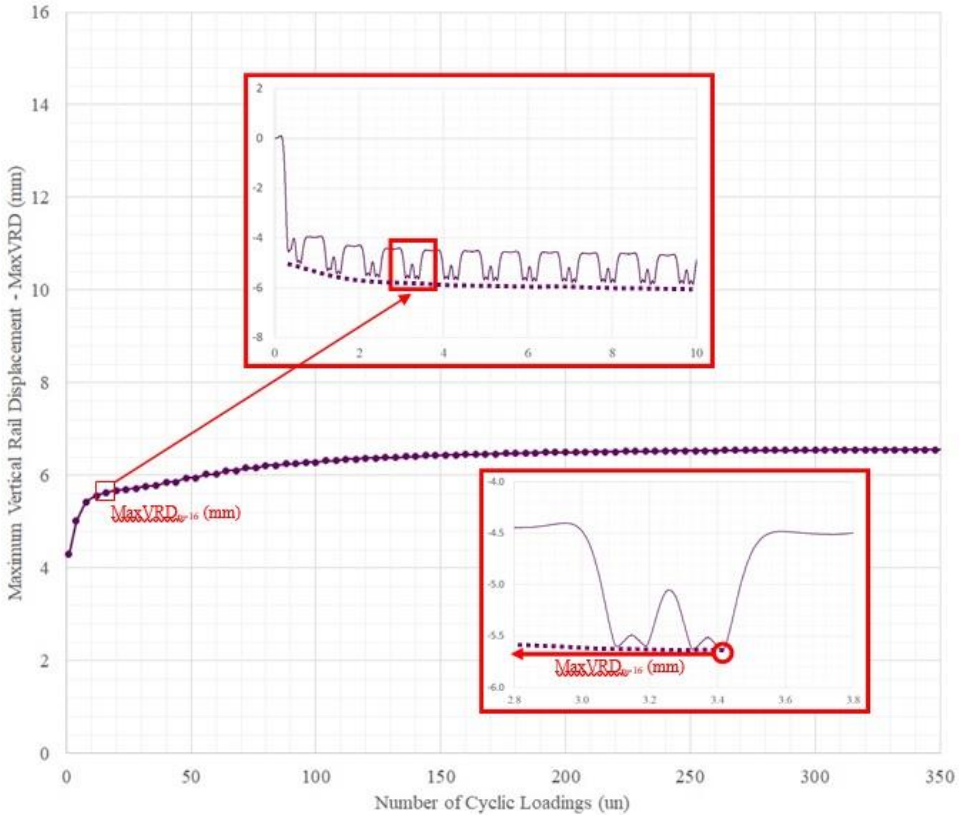

Fig. 10. Short-term behaviour of Max_{VRDs} after each 4-cyclic loading (a half loop) on FEM under 20-tonnes axle load, 70-km/h train velocity and 500-N/mm ballast tangent stiffness (in details, top: the vertical rail displacements, and bottom: the Max_{VRD} after the 16th load cycle).

Upon initial investigation, the outcomes of the FEM analysis in the previous step (short-term cyclic loadings) are collected to be input into a regression performance. During this stage, the maximum values of VRD (Figure 10), under cyclic loadings (short-term), are regressed by a Napierian logarithmic (LN) function to provide an estimation of the maximum VRD for real cyclic loadings as stated before. The coefficient of determination, denoted R^2, of LN expression, under 20-tonnes axle load, 70-km/h train velocity and 500-N/mm ballast tangent stiffness is 0.9640, indicating reasonably that the FEM results can be replicated by the nonlinear model to the prediction of future outcomes. The results for this step are shown in Figure 11 where there are two different coefficients: a_{VRD} and b_{VRD}. For the LN function, over 4+ cyclic loadings, the 1st coefficient (a_{VRD}) indicates in which rate the VRD rises when increases axle load, whilst the 2nd one (b_{VRD}) is related to the initial VRD, both of them intrinsically related to the 20-tonnes axle load. The result for a_{VRD} and b_{VRD} are 0.3489 and 4.6142 mm, respectively, and can be written as follows:

$$Max_{VRD}\,(20\text{-tonnes, }70\text{-km/h, }500\text{-N/mm}) = 0.3489*\ln(N) + 4.6142 \qquad (3.1)$$

where ‘MaxVRD(20-tonnes, 70-km/h, 500-N/mm)’ is the maximum vertical rail displacement under 20-tonnes axle load, 70-km/h train velocity and 500-N/mm ballast tangent stiffness, and ‘N’ is the number of cyclic loadings.

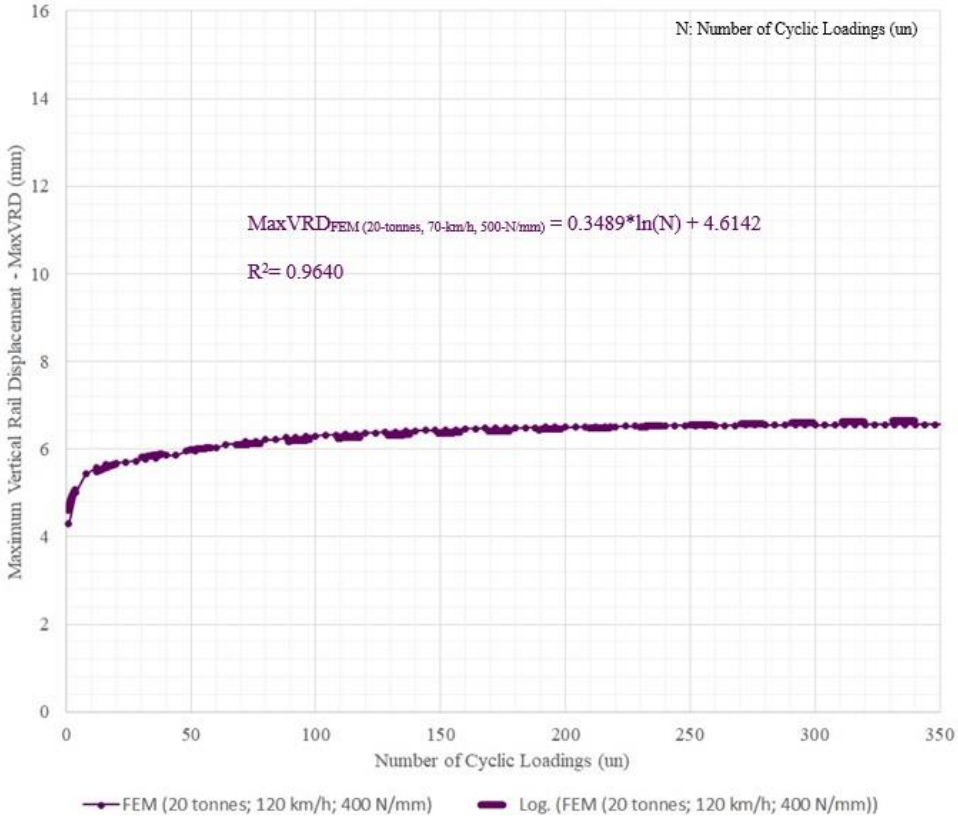

Fig. 11. Regression performance in the short-term behaviour of Max_{VRDs} after each 4-cyclic loading (a half loop) on FEM under 20-tonnes axle load, 70-km/h train velocity and 500-N/mm ballast tangent stiffness.

Following on the proposed methodology, the differences between each 4-cycle loads for a long-term behaviour (initially, < 6 MGT or 300 thousand cycle loads) of the Max_{VRD} LN function are calculated. The result indicates the first term of that regressed expression (Eq. 3.1) as the vertical levelling loss (VLL) of track geometry. Therefore, the track geometry VLL for those railway operation and track conditions can be written as:

$$VLL\ (20\text{-tonnes, 70-km/h, 500-N/mm}) = 0.3489*ln(N) \quad (3.2)$$

$$VLL\ (20\text{-tonnes, 70-km/h, 500-N/mm}) = 0.3489*ln(T/20) \quad (3.3)$$

where 'VLL (20-tonnes, 70-km/h, 500-N/mm)' is the vertical levelling loss (in mm) under 20-tonnes axle load, 70-km/h train velocity and 500-N/mm ballast tangent stiffness, 'N' is the number of cyclic loadings, and 'T' is million gross tonnes (MGT).

Eq. 3.2 provides an estimation of the cumulative VLL for the real cyclic loadings. That result is also compared to a robust triaxle experiment[43] under repeated loadings carried out by Ref. 32 under similar operational and track characteristics (20-tonnes axle load, 70-km/h train velocity and 500-N/mm ballast tangent stiffness – well-compacted crushed ballast) as aforementioned. Figure 12 shows the comparison of VLLs provided by the numerical (FEM and regression analytics) and the laboratory studies. It can be seen that the hybrid model gives a reasonable match with the measured data in the triaxle test, particularly after 50 thousand cycles. The VLL for 300 thousand cyclic loadings is approximately 4.5 mm on both methods. According to the benchmark models (Ref. 17 and Ref. 18), it also implies that the VLL in this study matches very well and falls within the well-compacted ballast track models (1-5 mm for 300 thousand cycles).

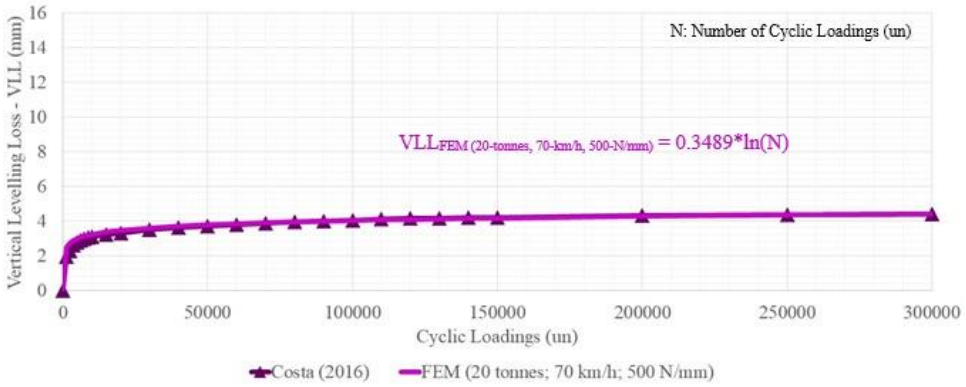

Fig. 12. Comparison of VLLs between the regression performance (from the numerical model – FEM) and the triaxle experiment carried by Costa (2016) – Ref. 32, under similar conditions (20-tonnes axle load, 70-km/h train velocity and 500-N/mm ballast tangent stiffness).

Additionally, different operational and track characteristics are applied to the verified model and the outcomes are compared to the studies provided by Ref. 39 and Ref. 41 taking into account similar conditions, respectively. Figure 13 depicts the comparisons of VLLs of our numerical study to those studies. It is noted that the FE model under 20-tonnes axle load, 120-km/h train velocity and 400-N/mm ballast tangent stiffness – medium-compacted crushed ballast – copes well with the Partington's investigation after 150 thousand cycles. Differ to the previous comparisons, the FE model under 30-tonnes axle load, 80-km/h train velocity and 350-N/mm ballast tangent stiffness (softer-compacted crushed ballast) conforms well to Indraratna's study (Ref. 41) even on the initial number of load cycles. The VLLs for 300 thousand cycles are 6.9 mm and 14.9 mm on both comparisons, respectively, indicating that the VLLs in these investigations are within medium and softer-compacted ballast track models, respectively (medium-compacted: 5-10 mm, and softer-compacted: 10-18 mm, for 300 thousand cycles, as described in Figure 3).

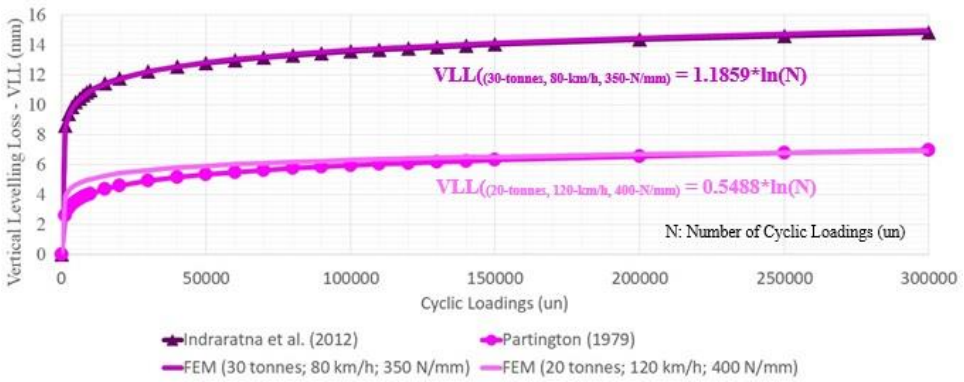

Fig. 13. Comparisons of VLLs between the regression performances (from the numerical model – FEM) and the studies carried out by Partington (1979) – Ref. 39 and Indraratna et al. (2012) – Ref. 41, under similar conditions, respectively (Partington: 20-tonnes axle load, 120-km/h train velocity and 400-N/mm ballast tangent stiffness; Indraratna: 30-tonnes axle load, 80-km/h train velocity and 350-N/mm ballast tangent stiffness).

In order to extend the validation of the model beyond 300 thousand cycles, the regression performance is applied under 3 million cyclic loadings or, approximately, 60 million gross tonnes (MGT) for 20-tonnes axle load. That amount of load represents roughly four months of traffic in a heavy haul railway in Brazil such as the EFC. The increase of VLLs of both investigations – Ref. 39 and Ref. 41 – and their similarities or contrasts with the FE models are shown in Figure 14. It can be seen that the FE model under 30-tonnes axle load continues to adjust well to Ref. 41's study (VLL = 17.7 mm and 17.4 mm, respectively, for 3 million cycles). Regarding the 20-tonnes FE model, it is identified a slight difference (approximately 1 mm) to Ref. 39's work (VLL = 8.2 mm and 9.3 mm, respectively, for 3 million cycles), meaning that it presents a reasonable match between them.

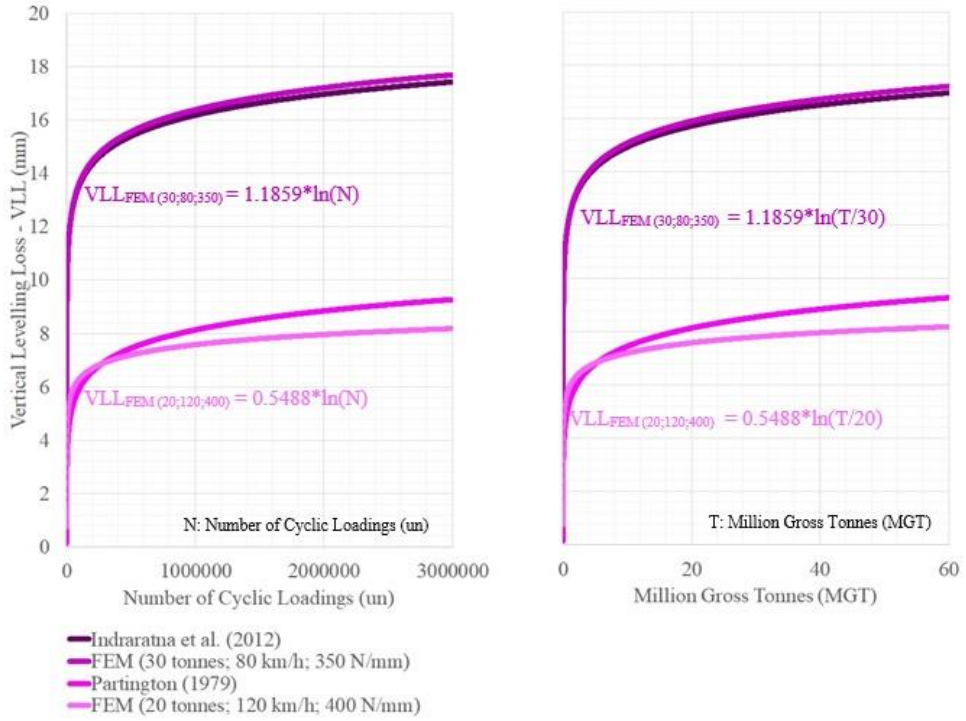

Fig. 14. Comparisons of VLLs between the regression performances (long-term) and the studies carried out by Partington (1979) – Ref. 39 and Indraratna et al. (2012) – Ref. 41 (left: < 3 M cycles; right: < 60 MGT).

From the previous comparisons undertaken between the FE models and other studies – Stage 3, it is possible to conclude that the proposed model can be validated and, consequently, applied to different railway dynamic conditions (including operation, vehicle, and track). The next stage is related to the track performance under key parameters, as indicated in Figure 7. It is mainly focused on varying those predefined parameters (axle load, train velocity and ballast tangent stiffness) onto the model to identify the rate of VLL and its behaviour, under cyclic loadings.

Similarly to Stage 3 – the model validation, in the Stage 4 numerical studies are performed and their outcomes are also extracted, analyzed, and regressed over LN functions. The 'a_{VLL}' coefficients of those VLL regression equations represent the rate in which that specific railway track under cyclic loadings loses its vertical levelling. In other words, those coefficients (a_{VLL}) simply mean how much, how faster, where and when those railway tracks are going to be degraded and, consequently, to have achieved their VLL thresholds (alert limit or intervention limit, as highlighted by Ref. 44). The rates of VLL (a_{VLL}) under the influence of ballast tangent stiffness and axle load are presented in Figures 15 and 16, respectively.

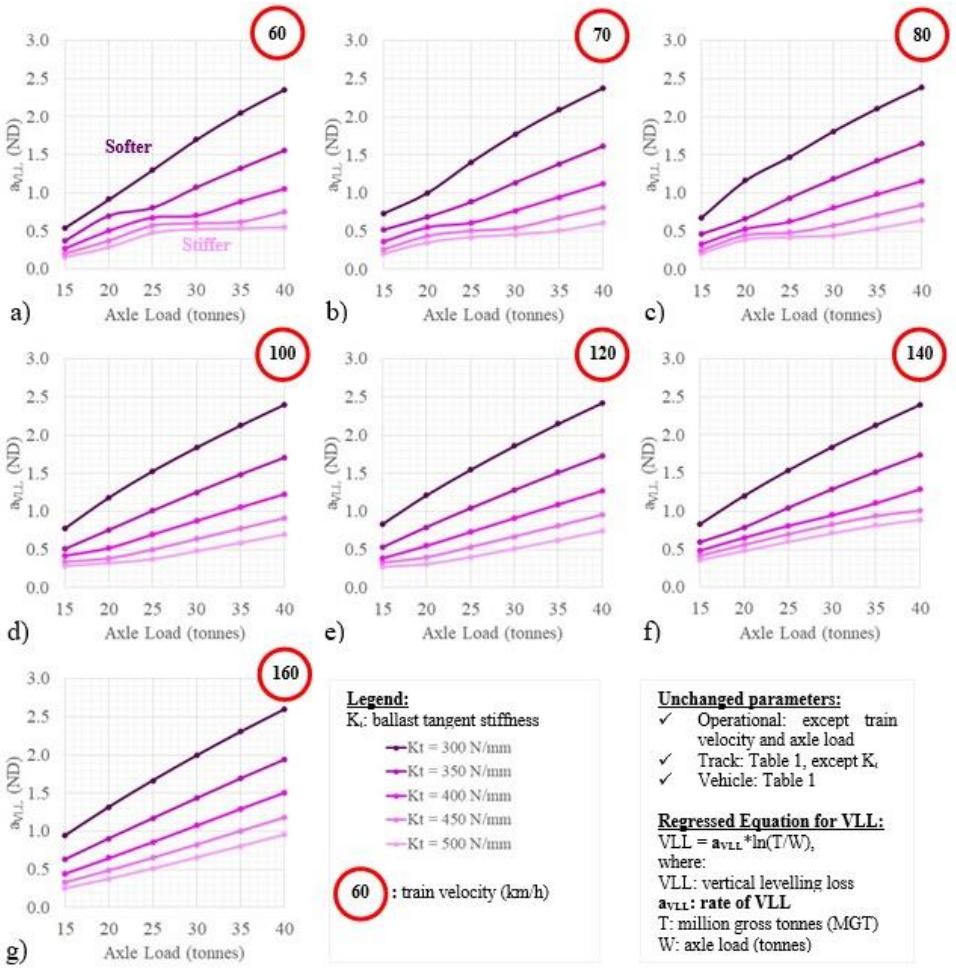

Fig. 15. 'a_{VLL}' coefficients in function of axle load under different ballast tangent stiffnesses (K_t) and train velocities.

For the railway tracks dominated by ballast tangent stiffness as shown in Figure 15, the rates in which the track geometry loses its vertical levelling climb considerably for low ballast tangent stiffness (softer ballast) – from 0.5 to 2.4 (500%) – when the axle load increases from 15 (light loads) to 40 tonnes (heavy haul loads), respectively, as expected, in an extreme situation. Those predictable accelerated degradations are intrinsically related not only to the contact force (axle load) but also to the high initial ballast void (loose ballast) applied into the track without a proper tamping (compaction). On the other hand, the 'a_{VLL}' coefficients for high ballast tangent stiffness (stiffer ballast) rise slightly or even maintain steadily, depending on both the axle load and the train velocity. As it can be observed, the rates increase from 0.2 to 0.5 between 15-tonnes and 25-tonnes axle loads, respectively, on low train velocity – 60 km/h (Figure 15a). Those coefficients maintain

steadily (around 0.5) between 25-tonnes and 30-tonnes axle loads on both 70-km/h and 80-km/h train velocities (Figure 15b and 15c), increase slightly (from 0.5 to 0.8) after 30-tonnes axle load on 100-km/h and higher train velocities (Figure 15d, 15e, 15f and 15g). In practice, this behaviour is anticipated since the well-compacted crushed ballast below the rail side sleepers has a reduced initial void causing the increase of ballast density and, consequently, its strength, also altering its natural frequencies. That observation further attests the findings presented by Ref. 45 and Ref. 46. Additionally, it is noted that, for example, on 70-km/h train velocity (Figure 15b), the rate of VLL raises from 0.4 to 0.6 (50%) if the axle load increases from 30 to 40 tonnes (30%), respectively – as intended by EFC (a heavy haul railway company) in Brazil, whose that kind of information might be taken into account to support the decision-maker.

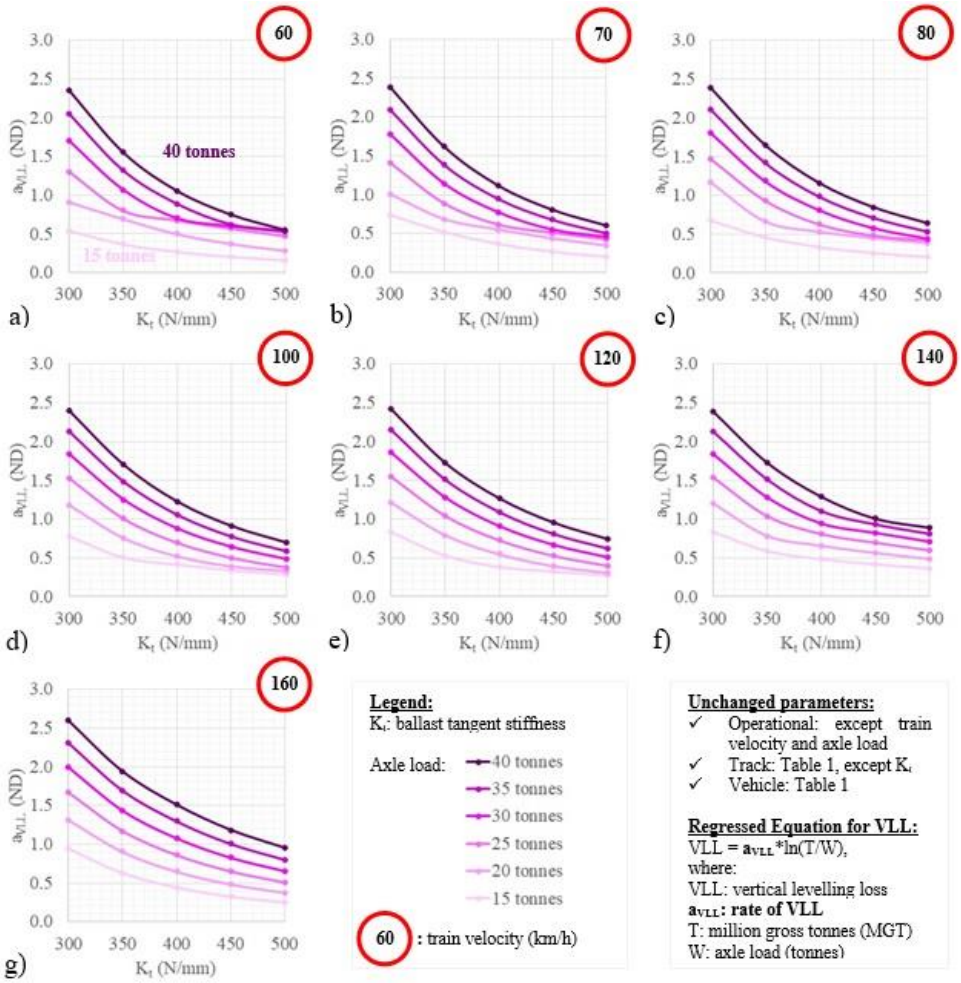

Fig. 16. 'a_{VLL}' coefficients in function of ballast tangent stiffness (K_t) under different axle loads and train velocities.

The rates of VLL can also be discussed looking into the axle load effect, as illustrated in Figure 16. The 'a_{VLL}' coefficients are plotted in function of ballast tangent stiffness for each established train velocity. A similar trend of VLL degradation can be found when either increase the ballast tangent stiffness or the train velocity indicating that the axle load plays an important role on track geometry degradation, as mentioned before. However, as it can be observed from Figure 16a, the influence of the axle load is reduced on 60-km/h train velocity for high ballast tangent stiffness showing a small increase of the rate (< 0.1) even when the axle load is boosted from 30 to 40 tonnes. It means that the wheel-rail contact force on 40-tonnes axle load, for example, has already explored the dynamic strength of a well-compacted crushed ballast over time. Also, Figure 16b, 16c, 16d, 16e and 16f depict that as faster as the train run, from 70 km/h to 140 km/h, the same behaviour can be identified – a small raise of the rate (< 0.1), although this behaviour moves onto the inferior neighbor axle load values as much as the train velocity increases (i.e. differ to 60-km/h train velocity, on 80-km/h train velocity and at high ballast stiffness – 500 N/mm, the 'a_{VLL}' rises slightly when the axle load increases from 20 to 25 tonnes). In fact, that behaviour is related not only to the axle load (contact force) but also to the natural frequencies of the railway track, as pointed out by Ref. 11. From Figure 16, it can also be seen that for softer ballast (at 300-N/mm ballast tangent stiffness), the command of axle load is evident though the rates of VLL behaviour indicates a variability depending on the train velocity.

In order to expand further the discussion regarding the influence of train velocity on the rate of VLL, Figure 17 is also presented. From the results shown in that Figure and in complement to the previous analysis, the 'a_{VLL}' coefficients do not present a straightforward tendency, generally, except when 40-tonnes axle load, 160-km/h train velocity and medium to softer ballast tangent stiffnesses are applied. This can be explained, according to Ref. 11, by the fact that each structure (i.e. a ballasted railway track) has its own natural frequencies, which affect the vertical displacement and, consequently, the VLL under cyclic loadings. Furthermore, the rate of VLL at 160-km/h train velocity and at 40-tonnes axle load for a 500-N/mm ballast tangent stiffness illustrated in Figure 17a (0.95) indicates 160 km/h or over as a possible critical velocity, which is likely to give a very high dynamic amplification and the effect of the load travelling speed can therefore be maximized. On the other hand, it is noted that at 60-km/h and 70-km/h train velocities, and at the same 25-tonnes axle load for the same medium ballast tangent stiffness (400-N/mm; Figure 17c), the rates of VLL are, respectively, 0.7 and 0.6, indicating that lower speed not necessarily means low rate of track geometry degradation. This observation also finds resonance in Ref. 10, Ref. 11, Ref. 12 and Ref. 13. Additionally, from Figure 17b, 17d, 17f, 17h and 17j, it is possible to note clearly the effect of train velocity on the rate of VLL, which, for example, presents high value (0.48) at 60-km/h train velocity and at 25-tonnes axle load for stiffer ballast (Figure 17b) if it is compared to 100-km/h (0.38), whereas for softer ballast (Figure 17j) at 25 tonnes and at 60 km/h and 100/km, the 'a_{VLL}' are 1.30 and 1.53, respectively. Therefore, it can be concluded that the influence of train velocity on track geometry VLL is naturally associated to the ballast parameters, particularly, in this

study, to the ballast tangent stiffness (K_t). Table 2 summarizes a_{VLL} coefficients for those track and operational conditions.

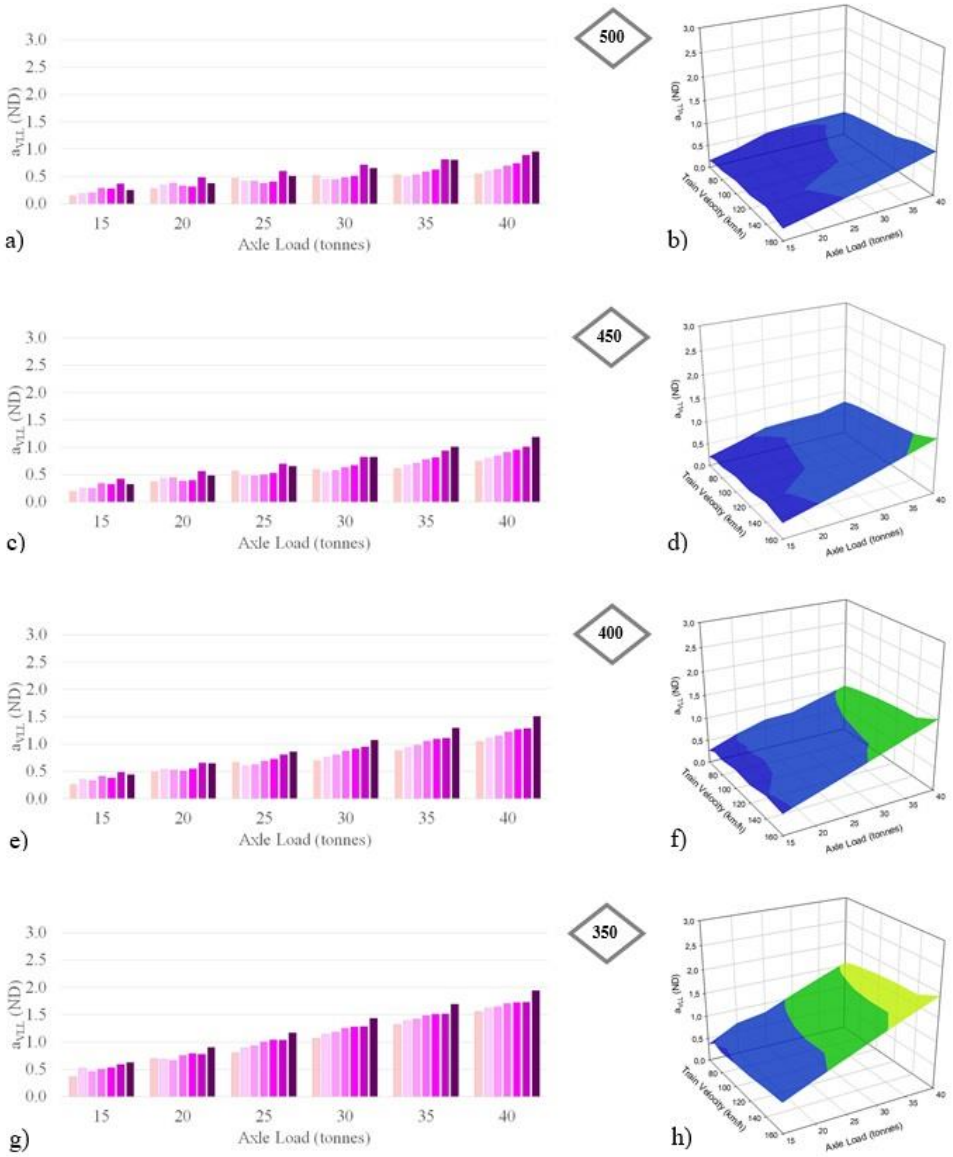

Fig. 17. A joint visualization of 'a_{VLL}' coefficients in function of the axle load under different train velocities and ballast tangent stiffnesses (top: stiffer ballast, and bottom: softer ballast tangent stiffness; left: axle load and train velocity in 2D view, and right: in 3D view) (continued)

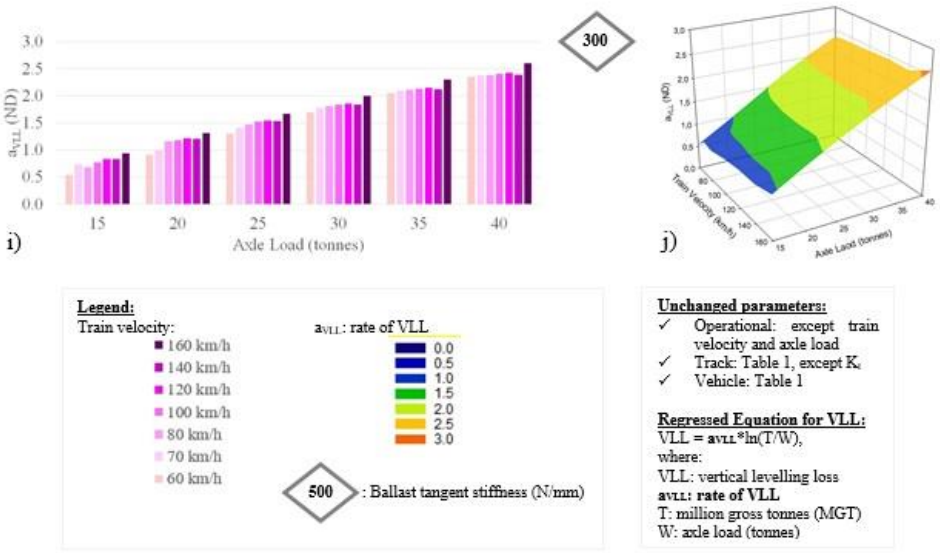

Fig. 17 (continued).

Table 2. A summary of a_{VLL} coefficients for particular railway track and operational conditions.

Kt (N/mm)	Axle load (tonnes)	Train Velocity (km/h)	a_{VLL} of LN function	Train Velocity (km/h)	a_{VLL} of LN function	Train Velocity (km/h)	a_{VLL} of LN function
300	15	60	0.5415	70	0.7322	80	0.6800
	20		0.9135		1.0035		1.1647
	25		1.3014		1.4091		1.4727
	30		1.6988		1.7758		1.8093
	35		2.0485		2.0956		2.1107
	40		2.3528		2.3829		2.3851
350	15	60	0.3662	70	0.5180	80	0.4627
	20		0.6959		0.6854		0.6653
	25		0.8024		0.8854		0.9359
	30		1.0702		1.1397		1.1859
	35		1.3188		1.3844		1.4249
	40		1.5558		1.6178		1.6504
400	15	60	0.2669	70	0.3655	80	0.3351
	20		0.5008		0.5524		0.5323
	25		0.6782		0.6114		0.6276
	30		0.7030		0.7704		0.8117
	35		0.8870		0.9464		0.9868
	40		1.0582		1.1193		1.1584
450	15	60	0.2034	70	0.2662	80	0.2568
	20		0.3744		0.4394		0.4516
	25		0.5715		0.5071		0.4833
	30		0.6027		0.5471		0.5801
	35		0.6218		0.6775		0.7134
	40		0.7535		0.8093		0.8459
500	15	60	0.1579	70	0.2019	80	0.2067
	20		0.2867		0.3489		0.3874
	25		0.4771		0.4196		0.4218
	30		0.5286		0.4532		0.4436
	35		0.5373		0.5035		0.5345
	40		0.5546		0.6062		0.6384

k_t: Ballast Tangent Stiffness; Ballast Elastic Stiffness (K_e): 45,430 N/mm; Ballast Yield Force (F_y): 500 N

Table 2 (continued).

Kt (N/mm)	Axle load (tonnes)	Train Velocity (km/h)	a_{VLL} of LN function	Train Velocity (km/h)	a_{VLL} of LN function	Train Velocity (km/h)	a_{VLL} of LN function	Train Velocity (km/h)	a_{VLL} of LN function
300	15	100	0.7728	120	0.8326	140	0.8347	160	0.9422
	20		1.1787		1.2121		1.2049		1.3178
	25		1.5278		1.5459		1.5354		1.6658
	30		1.8386		1.8587		1.8426		1.9947
	35		2.1283		2.1520		2.1273		2.3051
	40		2.4034		2.4264		2.3936		2.6005
350	15	100	0.5037	120	0.5302	140	0.5898	160	0.6297
	20		0.7531		0.7941		0.7827		0.9054
	25		1.0073		1.0424		1.0400		1.1708
	30		1.2518		1.2808		1.2836		1.4350
	35		1.4849		1.5105		1.5126		1.6934
	40		1.7058		1.7284		1.7311		1.9423
400	15	100	0.4148	120	0.3849	140	0.4855	160	0.4440
	20		0.5157		0.5488		0.6540		0.6493
	25		0.6947		0.7285		0.8100		0.8608
	30		0.8748		0.9104		0.9479		1.0779
	35		1.0532		1.0911		1.1074		1.2970
	40		1.2239		1.2670		1.2915		1.5097
450	15	100	0.3434	120	0.3272	140	0.4187	160	0.3273
	20		0.3876		0.3966		0.5606		0.4850
	25		0.5027		0.5305		0.6990		0.6516
	30		0.6378		0.6694		0.8268		0.8271
	35		0.7743		0.8102		0.9370		1.0066
	40		0.9094		0.9523		1.0084		1.1837
500	15	100	0.2906	120	0.2768	140	0.3643	160	0.2526
	20		0.3282		0.3123		0.4822		0.3767
	25		0.3793		0.4022		0.6018		0.5105
	30		0.4820		0.5094		0.7140		0.6547
	35		0.5894		0.6220		0.8165		0.8028
	40		0.6972		0.7388		0.8916		0.9513

k_t: Ballast Tangent Stiffness; Ballast Elastic Stiffness (K_e): 45,430 N/mm; Ballast Yield Force (F_y): 500 N

4. Conclusions

This study presents new insights into the importance of track geometry degradation after construction or maintenance activities. It highlights that the increasing demand for more-frequent railway transport accelerates the track degradation mainly by the differential track settlement. It affects directly on the spatial position of the railway track (track geometry), particularly, the vertical levelling.

To investigate this phenomenon, a numerical study is carried out focusing on the vertical levelling loss (VLL) of the track geometry. This loss is occurred in two phases during the track life, being the first directly after track construction or maintenance, under a rapid consolidation of the ballast. The second phase, largely also depending on ballast settlements, occurs in the short-term performance of which the rate can be approximately a linear degradation with the logarithm of the number of cyclic loadings including, as coefficients, the depended variables related to axle loads, train velocities and ballast tangent stiffness. Underpinning on that short-term performance, it is possible to extent the VLL prediction to evaluate its long-term behaviour following its regression function. It shows that the proposed numerical model is able to consider, as input, different operational, track and vehicle parameters to predict the VLL of the railway tack geometry.

Therefore, given that this hybrid approach can very well predict the VLL long-term performance considering not only the number of cycles or million gross tonnes (MGT) but also the different dynamic conditions, their findings contribute to obtain new insights regarding track geometry degradation and support the development of a specification to the proceeding. With the increase in computing power and speed, it will be possible to elaborate even more complex analysis of track geometry elements with a minimal need of carrying out expensive field experiments. Further research will focus on a non-linear elastic-plastic behaviour not only to ballast, but also to sub ballast and subgrade, and extend the studies to other track geometry components such as lateral alignment, cant and twist, on curve segments. This aspect is crucial when the formation is constructed over a soft soil where it can experience large strains.

Acknowledgments

The first author gratefully appreciates the Brazilian National Council for Scientific and Technological Development (CNPq), Brazil, Project No. 200359/2018-5, for his Ph.D. scholarship. We are sincerely grateful to the European Commission for the financial sponsorship of the H2020-RISE Project No. 691135 “RISEN: Rail Infrastructure Systems Engineering Network,” which enables a global research network that tackles the grand challenge of railway infrastructure resilience and advanced sensing in extreme environments.[47]

References

1. Y. Guo and W. Zahi, Long-term prediction of track geometry degradation in high-speed vehicle-ballastless track system due to differential subgrade settlement, *J. Soil Dynamics and Earthquake Engineering,* **113** (2018) 1–11.

2. J. C. O. Nielsen and X. Li, Railway track geometry degradation due to differential settlement of ballast/subgrade – Numerical prediction by an iterative procedure. *J. of Sound and Vibration* **412** (2018) 441–456.
3. N. H. Thom and J. Oakley, Predicting differential settlement in a railway trackbed, in *Proc. of Railway Foundation – RailFound 06*, Birmingham, United Kingdom (September 2006), pp. 190–200.
4. W. W. Hay, *Railroad Engineering* (2nd Edition, Wiley-Interscience, New York, 1982).
5. L. H. Hungria, *Segurança Operacional de Trens de Carga* (All Print, *São Paulo*, 2017) (in Portuguese)
6. BS-EN-1348-1, *Railway applications - Track - Track geometry quality – Part 1: Characterization of track geometry* (BSI Standards Publication, London, 2019).
7. B. Indraratna, W. Salim and C. Rujikiatkamjorn, *Advanced Rail Geotechnology – Ballast Track* (CRC Press, Florida, 2018).
8. E. T. Selig and J. M. Waters, *Track Geotechnology and Substructure Management* (Thomas Telford, London, 1994).
9. K. Nguyen, D. L. Villalmanzo, J. M. Goicolea, and F. Gabaldon, A computational procedure for prediction of ballasted track profile degradation under railway traffic loading, *J Rail and Rapid Transit* **230**(8) (2016) 1812–1827.
10. H. G. Kempfert and Y Hu, Measured dynamic loading of railway underground, in *Proc. of the 11th Pan-American Conf. on Soil Mechanics and Geotechnical Engineering*, Foz do Iguaçu, Brazil (November 1999), pp 843–847.
11. C. Esveld, Modern Railway Track (2nd Edition, MRT-Productions, Zaltbommel, 2001).
12. Q. Sun, Q, An Elasto-Plastic Strain-Based Approach for Analysing the Behaviour of Ballasted Rail Track (Thesis, University of Wollongong, Wollongong, 2015).
13. S. B. Mezher, D. P. Connolly, P. K. Woodward, O. Laghrouche, J. Pombo, and P. A. Costa, Railway critical velocity – Analytical prediction and analysis. *J. Transportation Geotechnics*, **6** (2016) 84–96.
14. J. Zakeri, M. Esmaeili and S. Mosayebi, Effects of sleeper support modulus on dynamic behaviour of railway tracks caused by moving wagon, *International Journal of Heavy Vehicle Systems* **24**(3) (2017).
15. J. Zakeri, M. Esmaeili and S. Mosayebi, Vehicle/track dynamic interaction considering developed railway substructure models, *Structural Engineering and Mechanics* **61**(6) (2017) 775–784.
16. J. Zakeri, M. Esmaeili and S. Mosayebi, Some aspects of support stiffness effects on dynamic ballasted railway tracks, *Periodica Polytechnica Civil Engineering* **60**(3) (2016) (https://doi.org/10.3311/PPci.7933).
17. T. Dahlberg, Some railroad settlement models – a critical review, *J Rail and Rapid Transit* **215**(4) (2001) 289–300.
18. I. Grossoni, A. R. Andrade, Y. Bezin, and S. Neves, The role of track stiffness and its spatial variability on long-term track quality deterioration. *J. Rail and Rapid Transit* **233**(1) (2019) 16–32.
19. M. Shenton, Deformation of railway ballast under repeated loading conditions, in AD Kerr (ed.) *Railroad Track Mechanics and Technology*, Princeton University, Pergamon, USA (July 1978).
20. N. Guerin, *Approche Experimentale et Numerique du Comportement du Ballast des Voies Ferrees* (Thesis, *Ecole Nationale des Ponts et Chaussees*, Paris, 1996) (in French).
21. H. E. Stewart. and E. Selif, Correlation of Concrete Tie Track Performance in Revenue Service and at the Facility for Accelerated Service Testing – Volume 2: Predictions and Evaluations of Track Settlement (Federal Railroad Administration, Report No. FRA-ORD-82/44.2, Washington DC, 1984).

22. T. Jeffs and S. Marich, Ballast characteristics in the laboratory, in *Conference on Railway Engineering*, Australia (August 1987).
23. B. Indraratna and W. Salim, Deformation and degradation mechanics of recycled ballast stabilised with geosynthetics, J. Soils Found **43** (2007) 35–46.
24. B. Indraratna and S. Nimbalkar, Stress-strain degradation response of railway ballast stabilized with geosynthetics, *J Geotech Geoenviron Eng* **139** (2013) 684–700.
25. J. P. Estaire and F. C. Vicente, CEDEX Track Box as an experimental tool to test railway tracks at 1:1 scale, *in Proc. of the 19th International Conference on Soil Mechanics and Geotechnical Engineering*, Seoul, South Korea (April 2017).
26. R. D. Frohling, Low frequency dynamic vehicle-track interaction: modelling and simulation. *J. Veh Syst Dyn* **29** (1998) 30–46.
27. V. Cuellar, Short and long-term behaviour of high-speed lines as determined in 1:1 scale laboratory tests, in *Proc. of 9th World Congress on Railway Research*, Lille, France (October 2011).
28. S. J. Blair and A. H. Chan, Modelling track deterioration – a brief review of past and current trends, in *Proc. of Railway Foundation – RailFound 06*, Birmingham, United Kingdom (September 2006), pp. 201–209.
29. C. Higgins and X. Liu, Modeling of track geometry degradation and decisions on safety and maintenance: A literature review and possible future research directions, *J. Rail and Rapid Transit* **232**(5) (2018) 1385–1397.
30. A. L. O. de Melo, S. Kaewunruen, M. Papaelias, L. L. B. Bernucci, and R. Motta, Methods to monitor and evaluate the deterioration of track and its components in a railway in-service: a systemic review. *J. Frontier Built Environment* **10** (2020).
31. C. Ngamkhanong, D. Li, A. M. Remennikov, and S. Kaewunruen, Dynamic capacity reduction of railway prestressed concrete sleepers due to surface abrasions considering the effects of strain rate and prestressing losses, *International Journal of Structural Stability and Dynamics* **19**(1) (2019) (https://doi.org/10.1142/S0219455419400017).
32. R. C. da Costa, *Proposição de Dispositivo de Medidas "in situ" para Avaliação do Comportamento Mecânico de Lastro Ferroviário: Estudo de Caso na Estrada de Ferro Carajás* (Dissertation, University of Sao Paulo, *São Paulo*, 2016) (in Portuguese).
33. R. C. da Costa, R. Motta, E. Moura, J. Pires, L. L. B. Bernucci, and L. Oliveira, Measuring device for in situ determination of the track modulus in a heavy haul track, in *Proc. of 11th International Heavy Haul Conference*, Cape Town, South Africa (June of 2017), pp. 101–110.
34. G. F. M. dos Santos, *Análise de Segurança de Veiculo Ferroviário de Carga em Tangente Considerando a Excitação Periodica da Via Permanente* (Thesis, University of Sao Paulo, *São Paulo*, 2015) (in Portuguese).
35. D. Li, J. Hyslip, T. Sussmann, and S. Chrismer, *Railway Geotechnics* (CRC Press, Florida, 2016).
36. LS-Dyna, *LS-DYNA® Keywords User's Manual – Volume 1* (Livermore Software Technology Corporation – LSTC, Livermore, 2014).
37. LS-Dyna, *LS-DYNA® Theory Manual* (LSTC, Livermore, 2019).
38. ORE (Office for Research and Experiments), *Stresses in the Rails, the Ballast and the Formation Resulting from Traffic Loads* (International Union of Railways, Question 71, Report No. 10, Volumes 1 and 2, Utrecht, 1970).
39. W. Partington, TM-TS-097: *Track Deterioration Study – Results of the Track Laboratory Experiments*, (British Railway Research, Derby, 1979).
40. T. Abadi, A review and evaluation of ballast settlement models using results from the Southampton Railway Testing Facility (SRTF). *Procedia Eng* **143** (2016) 999–1006.
41. B. Indraratna, N. T. Ngo and C. Rujikiatkamjorn, Deformation of coal fouled ballast stabilized with geogrid under cyclic load. *J. Geotech. Geoenviron. Eng.* **139**(8) (2012) 1275–1289.

42. Y. Sato, Japanese studies on deterioration of ballasted track, in Interaction of Railway Vehicles with the Track and its Substructure, *J. Vehicle System Dynamics Supplement* **24** 197–208 (Taylor & Francis, New York, 1995).
43. A. H. M Merheb, *Análise Mecânica do Lastro Ferroviário por Meio de Ensaios Triaxiais Cíclicos* (Dissertation, University of Sao Paulo, *São Paulo*, 2014) (in Portuguese).
44. BS-EN-1348-5, *Railway applications - Track - Track Geometry Quality – Part 5: Geometric Quality Levels - Plain Line, Switches and Crossings* (BSI Standards Publication, London, 2017).
45. E. Tutumluer, Y. M. A. Hashash, J. Ghaboussi, Y. Qian, S. J. Lee, and H. Huang, *Discrete Element Modeling of Railroad Ballast Behavior* (Report-No. DOT/FRA/ORD-18/20, Washington DC, 2018).
46. C. D. Foster and S. Kulkarni. Coupled multibody and finite element modelling of track settlement. In M. Barla, A. Di Donna and D. Sterpi (eds) Challenges and Innovations in Geomechanics. IACMAG 2021. *Lecture Notes in Civil Engineering*, **126** (2021).
47. S. Kaewunruen, J. M. Sussman and A. Matsumoto, Grand challenges in transportation and transit systems. J. Front. Built Envir. 3:6 (2016) (doi: 10.3389/fbuil.2016.00004).